High resolution x-ray and -ray imaging using a scintillator-coupled electron-multiplying CCD

High resolution X-ray and γ-ray imaging using a scintillator-coupled Electron-Multiplying CCD

David Hall* and Andrew Holland
e2v centre for electronic imaging, PSSRI, The Open University, MK7 6AA, UK

ABSTRACT

Over the last decade the rapid advancements in CCD technology have lead to significant developments in the field of low-light-level, Electron-Multiplying CCDs (EM-CCDs). The addition of a gain register before output allows signal electrons to be multiplied without increasing the external noise. This low effective readout noise, which can be reduced to the sub-electron level, allows very small signal levels to be detected. Caesium iodide is one of the most popular scintillation materials due to its many desirable properties. Approximately 60 photons are produced per keV of incident X-ray or γ-ray with wavelengths peaking at 550 nm (dependent on doping), matching the peak in the quantum efficiency of the back-illuminated CCD97 of over 90%. Using a scintillator coupled to an EMCCD it is possible to resolve individual interactions inside the scintillator. Multiple frames can be taken in quick succession with hundreds of interactions per frame. These interactions can be analysed individually using sub-pixel centroiding and the data compiled to create an image of a much higher resolution than that achieved with a single integrated frame. The interaction mechanism inside the scintillator is discussed with relation to the spatial and spectral resolution of the camera system. Analysis of individual events opens up the possibility of energy discrimination through the profiling of each interaction.

Keywords: photon-counting, EM-CCD, scintillator, imaging, spectroscopy, fluorescence

1. INTRODUCTION

Impact ionisation is a naturally occurring phenomenon in silicon when an electron passes through a region of high electric field. The electron can gain sufficient kinetic energy to effectively slam into the lattice and release further electrons. This process of impact ionisation increases unwanted charge in a CCD. The process can, however, be controlled, and it is through the controlled application of this process that the Electron Multiplying Charge Coupled Device (EM-CCD) operates. The EM-CCD is similar in many ways to the standard CCD, but includes an additional multiplication, or gain, register following on from the standard readout register. Through the application of a higher voltage to specific electrodes (typically 40-50 V) the impact ionisation can be controlled. By multiplying the signal electrons before readout it is possible to reduce the readout noise relative to the signal, effectively reducing the readout noise to the sub-electron level. With the application of sufficient gain it is possible to see very low-light-level signals.[1]

A scintillator can be added to the EM-CCD to allow much more efficient detection of hard X-rays. When an X-ray interacts in the scintillator it produces many photons at visible wavelengths. These photons pass through the scintillator to the CCD, spreading out radially from the initial point of interaction. The width of the spread of the light is dependent upon the depth of the interaction in the scintillator; the further the photons have to travel to the CCD the greater the spread. The spread of light in the scintillator leads to a degraded resolution when taking an integrated image. One method of improving the resolution involves the technique of photon-counting.

Further author information: send correspondence to David Hall, d.j.hall@open.ac.uk +44 (0)1908 332769
Address: e2v centre for electronic imaging, PSSRI, The Open University, Walton Hall, MK7 6AA, UK

Each X-ray interacting in the scintillator leaves a Gaussian-like signal profile at the EM-CCD with a peak signal of only a few photons. Through the use of a scintillator coupled to an EM-CCD running at an appropriately high frame-rate it is possible to resolve individual X-ray interactions in the scintillator. The analysis of the individual interactions opens the door to photon-counting and the centroiding of events to improve the spatial resolution achieved. Further investigation of the event profiles can provide information on the energy of the incident X-ray or electron. Through the analysis of individual events this study discusses the implications of secondary interactions and their effect on the image quality.

Following an outline of the detector and experimental layout, this paper presents results which have a critical impact on the imaging capabilities of such a detector and methods by which these problems may be overcome, significantly enhancing the image quality. The Modulation Transfer Function (MTF) shows great improvements using the photon-counting technique over the standard integration method.

Such a device is open to any industry or research requiring high frame-rate, high-resolution, hard X-ray imaging. Possible uses include medical imaging (such as SPECT and sentinel node imaging), synchrotron research (such as X-ray diffraction experiments) and security imaging.

2. THE DETECTOR

The detector used in this study is based around a scintillator coupled EM-CCD. The EM-CCD (Figure 1, left) is described in section 2.1 and is an e2v CCD97 with a fibre-optic plate bonded to the surface of the image region. The scintillator is described in section 2.2. CsI(Tl) was chosen for this study due to its many highly desirable properties and ease of columnar growth from a fibre-optic plate (Figure 1, right). The scintillating layer fibre-optic plate can be sandwiched to the EM-CCD fibre-optic plate, forming the device described here. The scintillator is not fixed to the EM-CCD, allowing the scintillator to be changed if required (such as a thicker scintillation layer for higher energy X-rays). The fibre-optic plates not only allow the passage of the visible light to the EM-CCD from the scintillator but will also absorb the incident X-rays not absorbed in the scintillator, minimising the possibility of direct detection. The experimental set-up is described in section 2.3 and although not optimised for device performance, it gives an indication of the properties of the device.

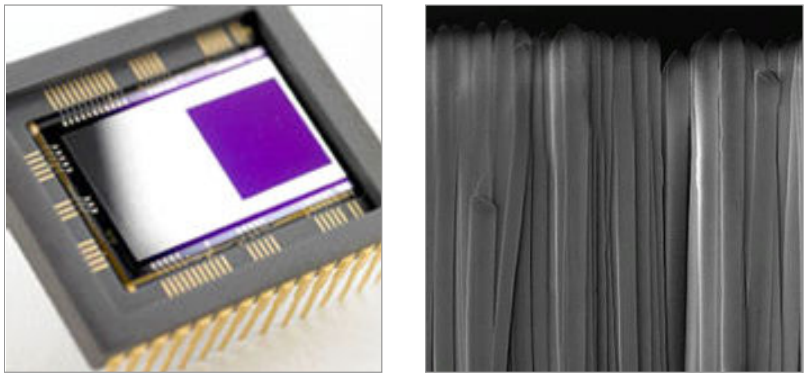

Figure 1. The EM-CCD used here is the e2v CCD97.[2]
The CsI(Tl) is formed of columns of diameter 5-6 µm.[3]

2.1 The Electron-Multiplying CCD

The EM-CCD is very similar to a standard CCD except for the addition of a gain register after the readout register (figure 2). Through the process of impact ionisation, electrons passing through the gain register generate further electrons by impact ionisation. As the signal is multiplied before readout, the effective readout noise can be reduced to the sub-electron level, making photon-counting possible with the low signal levels emitted from the scintillator.[1]

The device used in this study is the e2v back-illuminated 2-phase IMO CCD97.[2] The CCD97 has an image area of 512 × 512 pixels of 16 µm square, giving an overall imaging area of approximately 1 cm^2. Further to the main image section, the device contains several dark reference rows/columns and a store section of equal size (figure 2). The gain register, shown in figure 2, curves back below the readout register to give the device a more compact profile. The gain register is required in order to see the very low peak number of photons from each event.

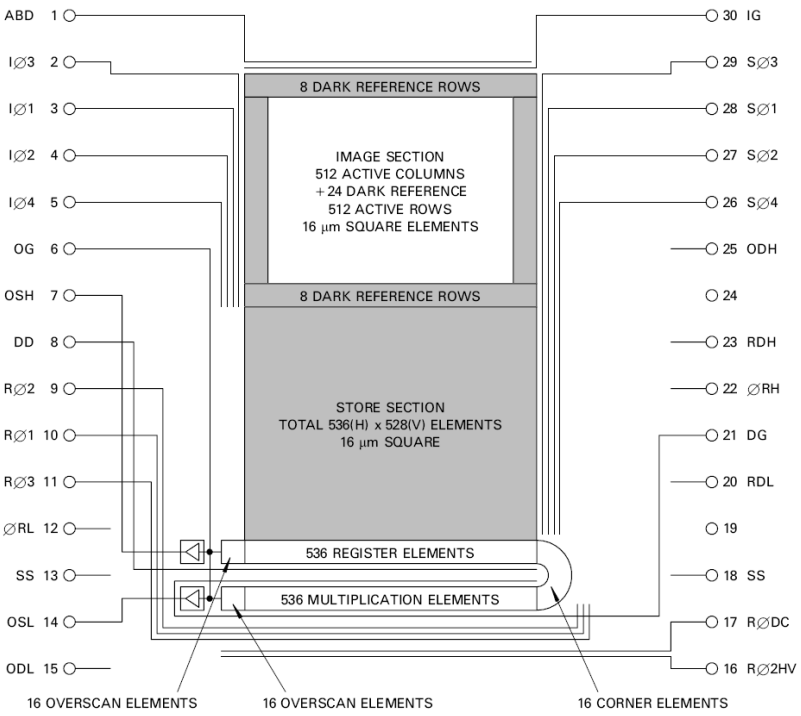

Figure 2. The layout of the CCD97 showing the readout register and additional gain register.[2]

2.2 Structured CsI(Tl)

High energy ionising electromagnetic radiation can be converted to photons of a lower energy through interaction with a scintillator. The energy can be absorbed and subsequently released in the form of many low energy photons as excited states relax.

CsI(Tl) has been chosen for this study due to its many highly desirable properties, including the high emission yield, the similarity of the refractive index to that of glass (for ease of coupling to a fibre-optic plate), low absorbance of the emitted lower energy photons and the ability to grow the scintillator in columnar form. If the scintillator is used in an unstructured form, the light spreads radially from the initial interaction point and the peak signal at the CCD is very low. To increase the peak number of photons reaching the CCD the scintillator can be grown in a columnar form (figure 1, right). The columnar structure acts in a similar way to a fibre-optic plate, channelling the light to the CCD. The scintillator is grown from the substrate and is not perfect in structure and does not cause perfect channelling of the lower energy photons, but it does act to increase the peak signal at the CCD. The peak wavelength of emission from the scintillator falls at 550 nm, matching the peak in quantum efficiency of the CCD97 of over 90%.

The scintillator produces approximately 60 photons per keV of incident energy, forming a linear dependence on energy over the range of interest. Through the analysis of the number of photons emitted it is in theory possible to relate this figure to the energy of the incident photons. It is not possible to relate the peak signal to the energy however, as the

depth of interaction in the scintillator has a large impact on the peak signal. The event profile of each X-ray interaction must be considered to approximate the energy of the incident photons. Again, the process is not simple as the interaction mechanisms in the scintillator must be considered (section 4).

2.3 Experimental set-up

The experimental set-up for the laboratory results presented here is shown in figure 3. A lab-safe solid source is positioned several centimetres from the mask to be imaged. The mask chosen here is that of a simple tungsten edge, placed at an angle of 2-3 degrees from the pixel edges. The mask is placed on the scintillator plate (scintillator coupled to fibre-optic plate), which is sandwiched against the fibre-optic plate of the customised CCD97.

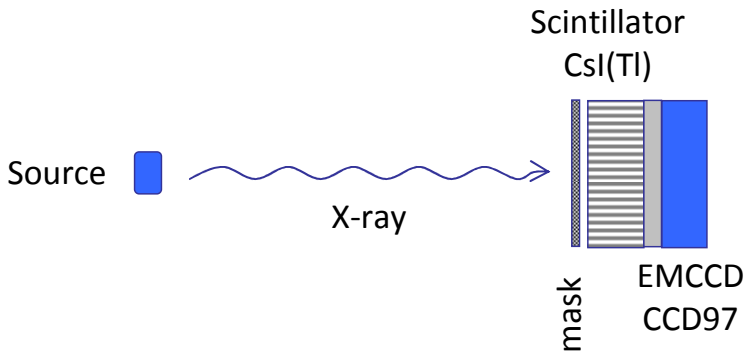

Figure 3. The experimental set-up, showing the radioactive source imaging the mask on the scintillator plate.

The set-up does not provide optimal measurements for the image quality, but has been used to demonstrate the principles involved. A parallel beam of X-rays is required to more accurately determine the Modulation Transfer Function (MTF) of the detector (section 3.3) and future synchrotron testing is hoped to provide such results. The divergence of the X-rays emitted from the solid source do not affect the spectral data (section 4), although the adverse effect on the MTF is thought to be significant.

3. PHOTON-COUNTING

Standard X-ray imaging techniques produce an integrated image: many X-ray interactions in the scintillator are taken for a single frame, producing the image in one snap-shot. Using this method, the spread of light in the scintillator is included in the image and it is not possible to post-process the image for removal of unwanted events. The resolution of such a detector is limited by the light-spread in the scintillator and by secondary event detection.

An alternative method of X-ray imaging involves the capture of multiple frames in quick succession, each containing several hundred X-ray interactions (figure 4). Each individual interaction can be seen as a Gaussian-like profile in the individual frames and the profiles are easily separable.

Through the analysis of each individual event profile it is possible to calculate the interaction position of the incident X-rays and to approximate the energy of the interaction. Centroiding each event profile provides a pin-point location for each interaction and negates the detrimental effects of the light spread in the scintillator. Further analysis of the event profiles can not only provide spectral information, but can also provide information as the interaction processes in the scintillator and the negative impact these can have on the image quality. Through a more detailed knowledge of the interaction mechanisms in the scintillator, one can consider methods to improve the detector MTF.

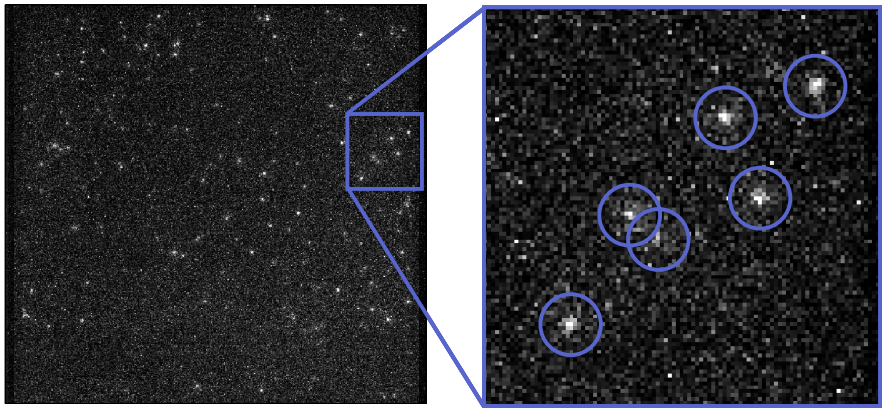

Figure 4. A full frame of approximately 200 individual event profiles is shown left. The enlarged section of the image (right) shows 6 individual Gaussian-like profiles, including possible re-absorption of fluorescence X-rays.

3.1 Point-search function

Once a frame has been captured, further processing is required to extract the event information. The background must be removed to create a level field-of-view. Following trials of various background removal techniques it was found that removing a single-value background based on the average signal level was the most effective. More complex background removal techniques cause inconsistencies around event profiles and require excess processing time, outweighing any positive impact. After the background removal, bright pixels were removed through consideration of relative signal levels between neighbouring pixels (bright pixels have an adverse effect on the event detection algorithms following smoothing).

Through the convolution of the image with an appropriate Gaussian kernel (with similar characteristics to the event profiles) the desired signal can be emphasised whilst efficiently suppressing noise in the image. The point-search function selects event profiles from the convoluted image which conform to the profile shown in figure 5.

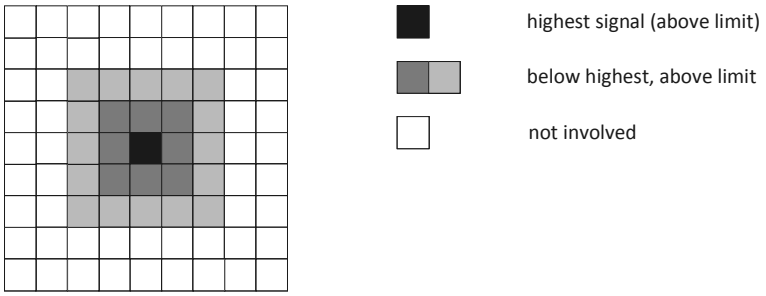

Figure 5. The point-search algorithm finds events in the convoluted image showing the form above.

The point-search function can be optimised through the variation of the smoothing kernel and the limits required for event detection. Taking a set of images of a solid edge and analysing the data with varying kernels and limits provides a set of two visualisations which can be used to select the most appropriate values for the required use (figure 6). The edge is placed covering approximately half of the image area. An integrated image is taken of the edge to determine the 'light' and 'dark' regions of the image. Alternatively, an image of the edge can be acquired optically using an LED.

The number of images used in the optimisation process can be varied, with an increase in the number of images chosen increasing the accuracy of the optimisation whilst also increasing the time-taken for the code to run.

The first plot (figure 6, left) shows the efficiency of the point-search function. The efficiency is defined as the fraction of detected events which are 'real' (i.e. caused by X-rays). The fraction of real events is given by equation 1, where *n* is the number of events and *A* is the area in pixels. This assumes that the detection of non-X-ray events is uniform across the CCD image area.

$$\text{Efficiency} = \frac{\left(\frac{n_{light}}{A_{light}}\right) - \left(\frac{n_{dark}}{A_{dark}}\right)}{\left(\frac{n_{total}}{A_{total}}\right)} \tag{1}$$

The second plot (figure 6, right) shows the number of 'real' events detected. The total number of real events detected is taken assuming that the number of non-X-ray events detected is uniform across the image area. As can be seen in figure 6, a compromise must be chosen. The maximum number of real events detected occurs with the minimum efficiency of detection – many real events are detected, but as a consequence, the percentage of total events that are real decreases. Conversely, a very high efficiency (highest percentage of real events) leaves a low number of real detections. For the testing here, a compromise was selected with 80% detection efficiency to increase the number of events per image and decrease run-times. The detection of non-events is uniform across the image area and does not have any major detrimental effects on the processing described here.

In order to more accurately optimise the point-search function, it is necessary to discount a region of pixels either side of the imaged edge. The results closest to the edge can be affected by fluorescence X-rays generated inside the scintillator which can pass underneath the edge into the 'dark' region of the image (internal fluorescence is discussed further in section 4).

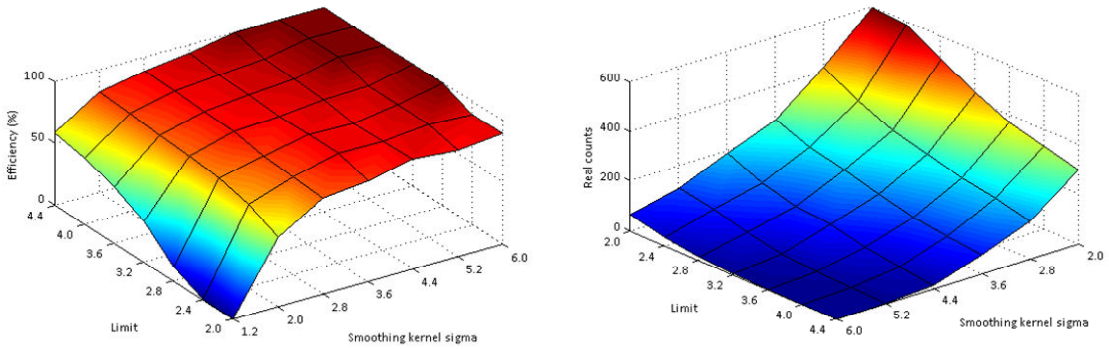

Figure 6. Point-search function optimisation: The efficiency (real events/total events) is shown to vary with smoothing kernel width and the signal limit (left). The number of real events is shown right.

3.2 Event profiles

The event profiles imaged with the EM-CCD can be analysed to reveal information about the origins of the incident X-rays. The Gaussian-like profiles can be centroided to provide sub-pixel locations for the interaction positions of the X-rays in the image plane. This improves the resolution very effectively over the standard integrated image.

Further information about the incident X-rays can be found through a deeper analysis of the events. One method of analysis, covered in previous studies,[4 5] involves the use of scale-selection in scale-space.[6 7 8] This provides a map of the events across peak intensity and event width. The map provides depth of interaction details of events in the scintillator, with those of greater width interacting further from the CCD. The map also provides details of the shape of the event profiles, showing a form which is Gaussian-like, but with a steeper fall-off. Finally, the map can be used to generate an energy spectrum of the events analysed.

This paper concentrates on a more basic method of energy determination using the summation of pixels surrounding the event peak. The central peak intensity cannot be used to generate energy data as the depth of interaction in the scintillator has a major effect on the peak intensity at any specific energy. A summation of 11 × 11 pixels (centred on the pixel of peak intensity) has been used to generate the spectra shown in section 4, effectively integrating below the Gaussian-like profile. This method requires much less processing time than the full scale-space approach, but does not portray the same quantity of information.

3.3 Imaging

The image quality provided by the detector has been assessed using the MTF edge technique.[9] A tungsten edges was placed at an angle of 2-3 degrees to the pixel edges across the image (figure 7). Multiple images were taken using a solid source in the arrangement detailed in figure 3. The images were used to generate both an integrated frame and a frame using the photon-counting technique, here grouping the pin-point locations to the nearest quarter-pixel. The images were sheared to shift the edge to the vertical and then summed to a single row, creating an oversampled Edge Spread Function (ESF), shown in figure 8 for both images.

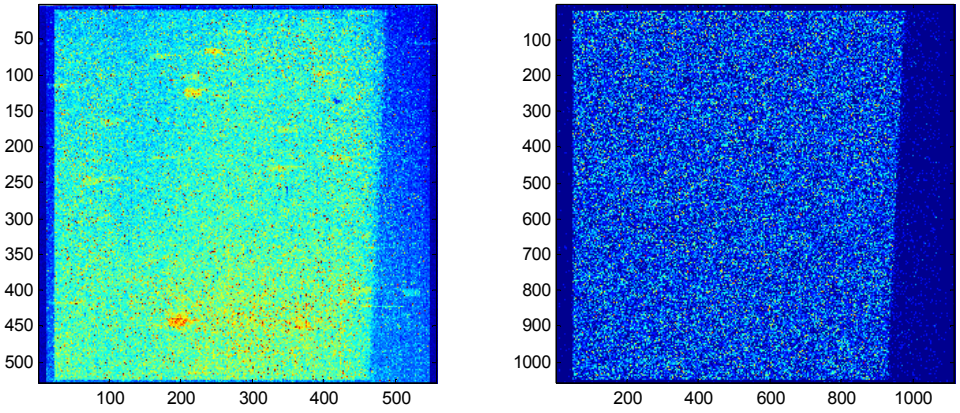

Figure 7. Edge images showing the integrated edge (left) and the photon-counted edge (right).

The ESF was binned to reduce some of the noise and differentiated to create the Line Spread Function (LSF) for each image. Due to the noise on the LSF and ESF, a curve was fitted to the data. The ESF and LSF were found to be noisy due to the low data count. To reduce the noise it would be necessary to acquire further frames. This was felt unnecessary for the purposes of this study.

The fitting of a Gaussian function to the LSF (as is often common practice) was found to be inappropriate, with little accuracy in representing the tails of the profile. The extended tails of the LSF were not due to the noise floor and it would be inaccurate and incomplete to extrapolate a Gaussian below these wings. A summation of two Gaussians was used to fit to the LSF. The fitted plots are shown as the LSF plots in figure 8, with the integrated functions shown against the corresponding ESF curves by the fine red line. It is the tails on the LSF curves which are of great interest when considering the imaging quality of the detector.

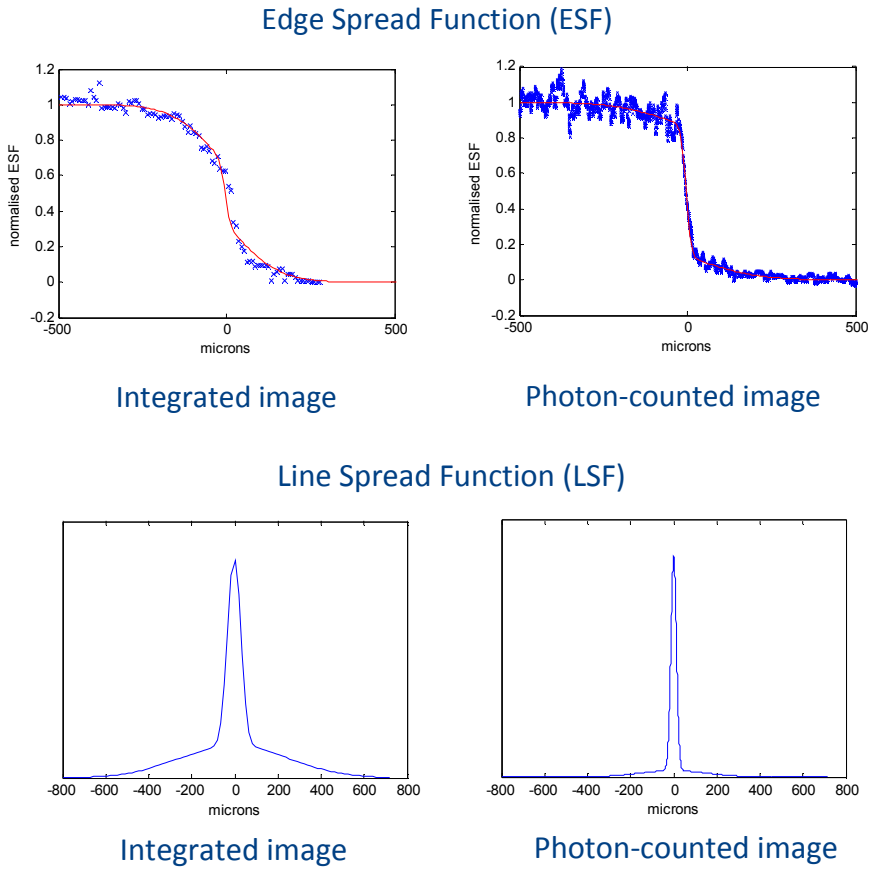

Figure 8. The ESF for the integrated and photon-counted images is shown top. The data points are shown as crosses with the fitted curve shown as the solid lines. The fitted curve was taken from integrating the fit to the LSF, shown bottom. The LSF follows the sum of two Gaussians of differing peak and width.

Taking the Fourier transform of the normalised, fitted LSF gives the MTF curves for both integrated and photon-counted images (figure 9). A step can be seen in the MTF, with the curve being formed from two parts. The steep drop in MTF at low frequencies is caused by the wings on the LSF. The slower decrease in MTF at higher frequencies is caused by the narrow central peak of the LSF.

The cause of the secondary Gaussian in the LSF has been investigated and has been found to be due to reabsorbed fluorescence in the scintillator. When an incident X-ray interacts in the scintillator, a K-shell caesium or iodine fluorescence X-ray can be emitted. This fluorescence X-ray can either leave the scintillator or be re-absorbed inside the scintillator layer and can be resolved with a high-resolution, low-light-level detector.[10] If the fluorescence X-ray is absorbed inside the scintillator a second event will be registered away from the initial interaction point. Events in close proximity, such as those overlapping in the lower left quadrant of figure 4, are attributed to an initial interaction and a reabsorbed fluorescence X-ray. Monte-Carlo simulations of the perfect device have shown how the fluorescence can 'creep' under the edge and into the dark region of the image, creating the tails seen in the LSF.

At first glance the integrated image LSF may appear to show greater fluorescence, but this is not the case. The LSF for the integrated image is consistent with the convolution of the photon-counted image LSF with a small Gaussian profile (based on the event profiles as shown in figure 4).

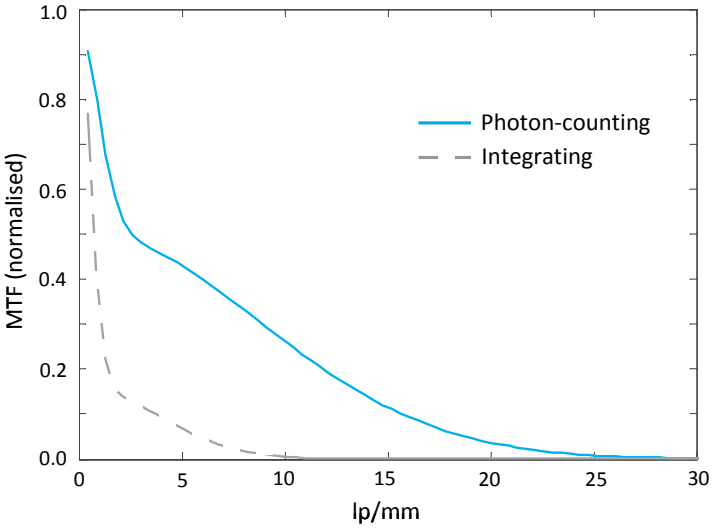

Figure 9. The MTF for the photon-counted and integrated images.

The MTF shown in figure 9 outlines the dramatic increase in MTF found by using the photon-counting method over the integrated method. The step in MTF, caused by the fluorescence creep, can be seen to have a much greater detrimental effect on the integrated image due to the higher peak of the secondary Gaussian seen in integrated image LSF. The MTF has been carefully normalised to ensure that the MTF shown in figure 9 is accurate. The LSF has been normalised before taking the Fourier transform, giving a definite MTF of unity at the lowest frequency without the need to approximate once the MTF curve has been produced.

4. SPECTRAL ANALYSIS

Using the summation method described previously, it is possible to analyse the individual event profiles and approximate the energy of the incident X-rays. The spectra produced give an insight into the interaction processes occurring inside the scintillator and allow some analysis of the effects of the reabsorbed fluorescence.

4.1 Americium-241

The Am^{241} source emits photons at 59.5 keV. Lower energy emitted photons are ignored by setting an appropriate limit on the point-search function for this testing. As can be seen in figure 10 (left), three peaks are present in the spectrum. The higher energy peak falls at 59.5 keV with FWHM of approximately 30%. The lower energy peaks are related to the K-shell X-ray fluorescence inside the scintillator. When an X-ray is generated the energy is transported away from the initial interaction location, leaving a lower energy event at the point of the initial interaction. If the fluorescence X-ray is re-absorbed then a second event is recorded at the energy of the fluorescence X-ray. This causes the two lower energy peaks seen in the spectrum. It is not possible to separate the two peaks using a 59.5 keV source due to the very small separation between the fluorescence X-ray energy and the energy remaining at the initial point of interaction.

4.2 Cobalt-57

The Co^{57} source emits photons at 14 keV, 122 keV and 136 keV. The emitted 122 keV component dominates over the emitted 136 keV component by a factor of nine, with further dominance due to the larger interaction cross-section in the scintillator at the lower energy. The highest energy peak in the spectrum (figure 10, right) is found at 122 keV, dominated by this component. At 14 keV a small peak can be found. With the larger interaction cross-section at 14 keV one might expect a larger peak, but the limit and smoothing kernel have been selected to concentrate on the higher energy events, losing the majority of the low energy events. The 14 keV events which are not removed through the point-search function are those found interacting near to the EM-CCD where the peak is high and the event width is small.

The three extra peaks present on the cobalt spectrum relate to the reabsorbed X-ray fluorescence and the energy remaining following fluorescence and secondary fluorescence. The complex spectrum provides complications when planning strategies to correct for the deterioration in MTF due to the fluorescence and electron motion.

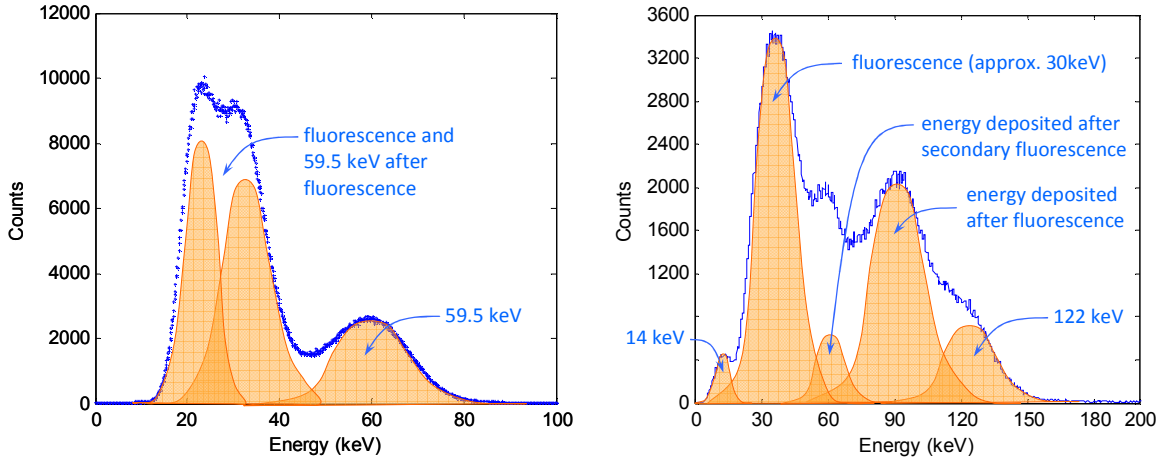

Figure 10. The spectra for Am^{241} (left) and Co^{57} (right) using the summation method. The Am^{241} source emits photons at 59.5 keV, whilst the Co^{57} source emits photons at 122 keV (87%), 136 keV (10%) at and 14 keV. Only the 14 keV photons interacting near to the CCD are detected at the limits set for the cobalt testing.

5. CONCLUSIONS

The MTF shows large improvements for the photon-counting mode over the integrating mode. Although the experimental set-up is not optimised for best-case MTF results, the resolution information obtained thus far shows great promise for the detector. Future high frame-rate testing at a synchrotron will provide much more accurate MTF measurements and will provide further insight into the effect of the internal fluorescence.

Following an investigation into the form of the LSF, it has been noted that fitting a Gaussian profile does not accurately portray the experimental data – simply extrapolating the main LSF peak overestimates the MTF by a factor of two in the photon-counting case detailed in this study and by a factor of five in the integrating mode results. Taking a single Gaussian peak ignores the impact of the fluorescence which is acting to degrade the MTF. The summed-Gaussian method uses a narrow width with a high peak to fit to the main LSF with a wider, lower peak to fit to the fluorescence. The two Gaussian profiles together create a stepped MTF. Decreasing the fluorescence component increases the MTF significantly. Such a move can be considered through splitting the events using the energy spectrum. This would, however, decrease the number of events or require larger run-times for equivalent data-sets. Preliminary splitting of the events by energy has shown increases in MTF of over 50%.

The use of a scintillator with a lower fluorescent yield would lead to a large increase in the MTF. The consideration of the fluorescent yield in scintillator selection for high-resolution imaging is an important one. Future work will cover scintillator choice and aim to investigate possible scintillators with lower fluorescent yields.

ACKNOWLEDGEMENTS

With thanks to David Burt, Mark Robbins, Peter Pool and Bill Bruns of e2v technologies, and to the members of the e2v centre for electronic imaging for their advice and support. Also with thanks to David Smith of Brunel University, for his help and advice in the preliminary work to this study.

REFERENCES

1. Jerram, P., Pool, P., Bell, R., Burt, D., Bowring, S., Spencer, S., Hazelwood, M., Moody, I., Catlett, N., Heyes, P., "The LLLCCD: Low light imaging without the need for an intensifier," *Proc. SPIE* **4306**, 178-186 (2001)
2. e2v CCD97 data-sheet, A1A-CCD97BI_2P_IMO Issue 3 (2004)
3. Private communication with Bill Bruns, e2v technologies
4. D. J. Hall, A. Holland, and D. R. Smith, "Imaging and spectroscopy using a scintillator-coupled EMCCD", *SPIE* **7021**, 70211Z (2008)
5. D. J. Hall, A. Holland, and D. R. Smith, "The use of automatic scale selection to improve the spatial and spectral resolution of a scintillator-coupled EMCCD", *NIM A* **604**, 207-210 (2009)
6. Lindeberg, T., "Discrete Scale-Space Theory and the Scale-Space Primal Sketch," PhD thesis, ISRN KTH NA/P--91/8-SE, all, (1991)
7. Lindeberg, T., "Feature detection with automatic scale selection," *International Journal of Computer Vision* **30**, no. 2, 77-116 (1998)
8. Lindeberg, T., "Principles for automatic scale selection", *Handbook on Computer Vision and Applications* **2**, 239-274, (1999)
9. E. Samei, M. J. Flynn, D. A. Reimann, "A method for measuring the presampled MTF of digital radiographic systems using an edge test device", *Med Phys.* **25**, 102–113 (1998)
10. Miller, B., W., Barber, H., B., Barrett, H., H., Shestakova, I., Singh, B., Nagarkar, V., V., "Single-photon spatial and energy resolution of a columnar CsI(Tl)/EMCCD gamma-camera using maximum-likelihood estimation," *SPIE* **6142**, 61421T (2006)